Journal of Engineering, Project, and Production Management
2026, 16(6), 2025-263

Cross-Border Fresh Product Transportation Optimization via Multi-Objective Models and Hybrid Algorithms

Zhe Chen[1] and Guangwen Zhang[2]
[1] Instructor, Digital Business College, Heilongjiang Polytechnic, Harbin, 150001, China,
[2] Instructor, Digital Business College, Heilongjiang Polytechnic, Harbin, 150001, China,
E-mail: zhangguangwen2025@163.com (corresponding author).

Production Management
Received November 10, 2025; revised January 26, 2026; accepted June 21, 2026
Available online July 2, 2026

Abstract: The transportation of cross-border fresh products is characterized by high time sensitivity and intense vulnerability to spoilage. However, most existing studies overlook the randomness of customs clearance, which limits the practical application of routing plans. Therefore, this study proposes a transportation route optimization model for cross-border e-commerce of fresh products based on multi-objective optimization and hybrid algorithms. It fully leverages the hunting mechanism of the Harris Hawks Optimization (HHO) algorithm to enhance local exploitation, and improves the inertia weight of the Particle Swarm Optimization (PSO) algorithm by predicting traffic congestion and customs delays using Weighted Random Forest (WRF). Experimental results show that the receiver operating characteristic curve of the proposed model is closest to the upper-left corner, with an area under the curve reaching 0.89, indicating better classification performance and predictive accuracy. The model also achieves F1 scores above 80%, with an annual average satisfaction rate of 92.2% for timelines. The average annual satisfaction rate for quality is 94.3%, 17.9% higher than that of the traditional weighted random forest algorithm. These results demonstrate that the proposed model achieves significant optimization performance in cross-border e-commerce fresh-product transportation scenarios. It effectively improves logistics efficiency and provides a multi-objective solution balancing cost and quality for the industry.

Keywords: Multi-objective model; hybrid algorithm; fresh products; route optimization; harris hawks optimization (HHO).

DOI 10.32738/JEPPM-2025-263

1. Introduction

In recent years, with the application of new insulation materials, breakthroughs in cold chain technologies such as intelligent temperature control systems, and the continuous improvement of international logistics networks, have enabled fresh products, once limited by short shelf lives, to reach global markets and support worldwide buying and selling scenarios (Bai et al., 2023). At present, cross-border e-commerce logistics for fresh products face challenges such as high transportation costs and high product loss rates (Wu et al., 2022). The core challenge lies in the dynamic variability of transportation networks and the significant randomness in the processing time of key nodes, which makes path planning extremely complex. However, existing research mainly focuses on single objective optimization or assumes static networks, lacking explicit modeling and real-time integration capabilities for random delay factors such as customs clearance, which cannot effectively balance cost, freshness, and delivery speed, resulting in insufficient robustness of theoretical solutions in practical applications (Fahrni et al., 2022; Plewes et al., 2023). Non-dominated Sorting Genetic Algorithm 2 (NSGA2) generates a well-distributed set of accurate Pareto-optimal solutions by introducing fast non-dominated sorting (He et al., 2023). Harris Hawks Optimization (HHO) simulates cooperative hunting behavior to achieve dynamic global optimization (Ryalat et al., 2023). Random Forest can effectively oversee high-dimensional logistics features by leveraging ensemble learning (Safia, 2023). Therefore, this study proposes a route optimization model that integrates NSGA2-HHO and Improved Particle Swarm Optimization with Weighted Random Forest (IPSO-WRF), aiming to provide an intelligent decision-making solution that combines global optimization capability with dynamic response speed for cross-border e-commerce fresh logistics. The core objective of this study is to develop a decision-making framework that simultaneously optimizes logistics costs, product freshness, and delivery timeliness. By explicitly modeling the randomness of customs clearance and dynamically integrating real-time data, the practicality and anti-interference ability of the path scheme can be effectively improved.

The innovation of this study lies in combining the NSGA2-HHO algorithm with the IPSO-WRF prediction module.

The former is responsible for searching for the Pareto-optimal set of paths in the global space. At the same time, the latter dynamically evaluates and fine-tunes the path at the minute level using real-time data, achieving a balance between static planning and dynamic adjustment. (2) Modeling the processing time as a log normal distribution based on historical data, and inputting the probability of customs clearance status as a key dynamic feature into the prediction model, enables path optimization to actively consider and adapt to such uncertainties. (3) By embedding HHO's biomimetic search mechanism into the NSGA2 multi-objective framework to enhance local development capabilities, and utilizing IPSO to optimize the weighted prediction process of WRF, the overall adaptability and solution accuracy of the algorithm in complex dynamic logistics scenarios are improved.

2. Related Works

Intelligent, algorithm-driven methods and multi-objective coordination have been applied across various fields, demonstrating strong potential to improve feature-extraction accuracy. Li et al. (2025) deployed a supporting system within a multi-objective optimization framework and adopted a global optimization method based on a multiscale quantum harmonic oscillator algorithm and genetic algorithm to explore how different algorithm models captured non-dominated solutions for interacting objective functions. Abeer et al. (2024) proposed a multi-objective latent space optimization method and improved the model's sampling efficiency in suggesting new molecules with enhanced characteristics through an iterative weighted retraining approach. Guizzo et al. (2023) developed a multi-objective evolutionary method that automatically generated finite-state machines from error reports written in natural language. The generated state machines were guided by a multi-objective evolutionary algorithm and benchmarked against baseline tools to evaluate software feasibility. Hussain et al. (2023) introduced a multi-objective optimization model to study vehicle fog computing networks that offload computing workloads from passenger devices onto traffic infrastructure. The solution generated optimal topologies based on the trade-off between service delay and energy consumption. Zhang et al. (2023) proposed a hybrid algorithm to score biomedical articles in a database using an improved BM25. The method then used a cluster-based summary extraction approach in a second phase to better identify and utilize relevant biomedical articles.

As transportation route optimization methods have developed, both theory and practical application have become increasingly mature. Ren et al. (2023) developed a mathematical model for dynamic, real-time vehicle routing problems in regional emergency material distribution. The model aimed to minimize vehicle routing costs, delay penalties, fixed vehicle costs, and total travel distance. Ru et al. (2024) constructed a multimodal vehicle logistics network and applied a graph traversal algorithm to identify feasible paths within it, thereby improving the profitability of vehicle logistics enterprises. Liu et al. (2023) proposed a novel method for optimizing real-world delivery routes using a language model. This approach learned from experienced drivers historical behavior and integrated that knowledge into the route-planning process. Dong et al. (2022) studied a joint optimization and visualization model for inventory transportation in agricultural logistics based on an ant colony algorithm. They introduced inventory-variation factors into the periodic vehicle-routing process to jointly optimize inventory decisions and route planning. Sang et al. (2023) proposed an improved directional A* algorithm to solve problems in traditional routing methods. By adding angular constraints to the evaluation function, the method transformed sharp turns into obtuse angles, enhanced distance functions to improve directional guidance, and removed redundant nodes to produce simpler route representations.

In summary, despite extensive research on route optimization, most existing studies on cross-border fresh logistics scenarios still lack explicit modeling of the randomness of customs clearance and other processes, which is disconnected from real-time perception capabilities, making it difficult to make closed-loop decisions in dynamic environments, and failing to achieve deep collaboration between global search, local fine-tuning, and real-time prediction. Therefore, this study proposes a transportation route optimization model for cross-border e-commerce fresh products, based on multi-objective optimization and hybrid algorithms, to address the above gap. Specifically, this study explicitly incorporates randomness into the optimization framework by introducing a probability distribution model of customs clearance time. Meanwhile, by constructing a collaborative mechanism between NSGA2-HHO and IPSO-WRF, dynamic data-driven real-time prediction and path re-optimization have been achieved. Through deep interaction among algorithm components, overall adaptability and decision robustness in complex, changing environments have been improved.

3. Multi-Objective Model and Hybrid Algorithm for Optimizing Cross-Border Product Transportation Routes

3.1. Multi-Objective Algorithm Design Combining NSGA2 and HHO

The optimization of cross-border fresh-food logistics paths is a low- to medium-dimensional, multi-objective optimization problem. Although NSGA3 performs better in high-dimensional objective space, its reference point-based selection mechanism has no significant advantage when the number of objectives is small, and instead increases computational complexity. NSGA2 can effectively maintain diversity and convergence of the solution set in the mid- to low-dimensional range through fast non-dominated sorting and crowding-distance calculation (Zhang et al., 2024). Therefore, this study selects NSGA2 to support cross-border logistics decision-making. The flowchart of the NSGA2 multi-objective algorithm is shown in Fig. 1.

As shown in Fig. 1, the NSGA2 algorithm begins by initializing the population, then performs non-dominated sorting and calculates crowding distances. Next, it generates a new generation through selection, crossover, and mutation. The new population is merged with the original population and then undergoes non-dominated sorting and crowding-distance calculation again. When comparing individuals in the merged population, the algorithm selects the individual with the lower dominance rank. If the ranks are equal, the one with the higher crowding distance is selected. After generating the new population, non-dominated sorting and crowding distance calculation are repeated. The equation for calculating the crowding distance of a middle individual in NSGA2 is shown in Eq. (1).

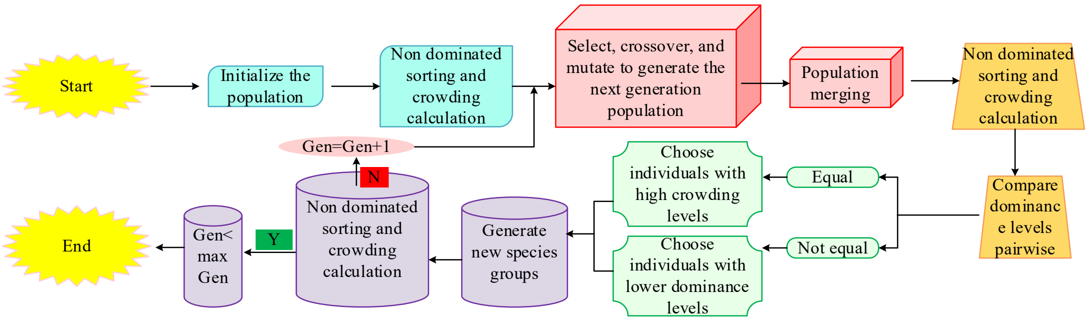

Fig. 1. NSGA2 multi-objective algorithm flowchart (source: author self-drawn)

$$CD_i = \sum_{m=1}^{M} \frac{f_m(i+1) - f_m(i-1)}{f_m^{\max} - f_m^{\min}} \tag{1}$$

In Eq. (1), M represents the objective function. $f_m^{\max}$ and $f_m^{\min}$ represent the extreme values of the m-th objective in the same layer. The crossover operation equation for NSGA2 is given by Eq. (2).

$$\begin{cases} y_1 = 0.5[(1+\beta)x_1 + (1-\beta)x_2] \\ y_2 = 0.5[(1-\beta)x_1 + (1+\beta)x_2] \end{cases} \tag{2}$$

In Eq. (2), x_1 and x_2 represent the parents, and y_1 and y_2 represent the offspring. The value β is defined in Eq. (3).

$$\beta = \begin{Bmatrix} (2u)^{1/(n_c+1)} & u \le 0.5 \\ (1/(2(1-u))^{1/(n_c+1)} & u > 0.5 \end{Bmatrix} \tag{3}$$

In Eq. (3), n_c denotes the crossover distribution index, which controls the similarity between parents and offspring. NSGA2 lays the foundation for multi-objective optimization by generating uniformly distributed Pareto solution sets through fast non-dominated sorting. Additionally, to enhance global search and local fine-tuning capabilities, the HHO algorithm is introduced. HHO simulates the cooperative hunting behavior of eagle swarms, effectively avoiding premature convergence by dynamically adjusting exploration and exploitation strategies. It is particularly suitable for transport route optimization problems with time-varying characteristics. The integration of NSGA2 and HHO not only leverages NSGA2's Pareto ranking to maintain the distribution of solution sets but also utilizes HHO's biomimetic search mechanism to improve convergence accuracy and speed, making it more applicable to dynamic multi-objective optimization scenarios such as cross-border fresh logistics. The HHO algorithm flowchart is shown in Fig. 2.

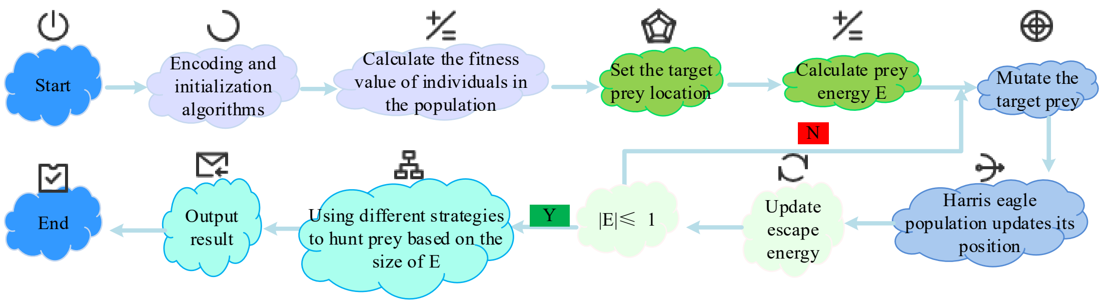

Fig. 2. HHO algorithm flowchart (icon source from: https://iconpark.oceanengine.com)

In Fig. 2, the HHO algorithm starts by initializing the population and parameters, then calculates the time set and population fitness. It sets the target prey, mutates it, and updates the hawk's position. The escape energy E is calculated to determine the pursuit strategy. The hawk's behavior is simulated to balance global exploration and local convergence. The position update equation during the exploration phase of HHO is shown in Eq. (4).

$$X(t+1) = \begin{cases} X_{rand}(t) - r_1 \,|\, X_{rand}(t) - 2r_2 X(t) & ifq \ge 0.5 \\ X_{rabbit}(t) - X_{avg}(t) - r_3(LB + r_4(UB - LB)) & ifq \ge 0.5 \end{cases} \tag{4}$$

In Eq. (4), $X(t)$ represents the current hawk position. $X_{rabbit}(t)$ denotes the position of the prey, or current optimal solution. $X_{rand}(t)$ is the randomly selected hawk position. $X_{avg}(t)$ is the average population position. r is a random number between 0 and 1. UB and LB represent the upper and lower bounds of the variables. The mathematical expression of escape energy E during the transition to the exploitation phase is shown in Eq. (5).

$$E = 2E_0(1-\frac{d}{D}) \tag{5}$$

In Eq. (5), E_0 represents the initial energy ranging from -1 to 1. d denotes the current iteration number, and D is the maximum number of iterations. If $|E| \geq 1$, the exploration continues. If $|E| < 1$, the algorithm shifts to exploitation. HHO strengthens local fine-tuning. NSGA2 ensures diversity and convergence in global search through non-dominated sorting and crowding distance. Therefore, this study combines NSGA2 and HHO into the NSGA2-HHO multi-objective algorithm. The flowchart is shown in Fig. 3.

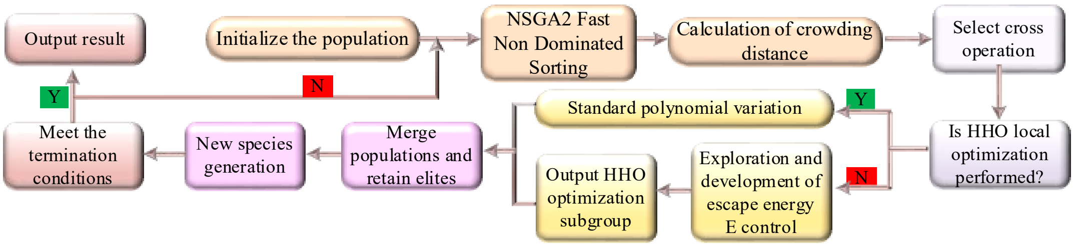

Fig. 3. Flowchart of multi-objective algorithm combining NSGA2 and HHO (source: author self-drawn)

In Fig. 3, the algorithm begins by initializing the population to generate initial solutions. It then performs NSGA2's fast non-dominated sorting to rank individuals by dominance. After selection and crossover operations generate new individuals, the algorithm enters the HHO phase. Escape energy E controls the balance between exploration and exploitation. If local optimization with HHO is not performed, standard polynomial mutation is applied. The two populations are then merged, and high-quality individuals are preserved through elitism. The soft encircling mathematical expression for energy E During the HHO exploitation phase, it is shown in Eq. (6).

$$X(t+1) = \Delta X(t) - E \mid JX_{rabbit}(t) - X(t) \tag{6}$$

The equation for $\Delta X(t)$ in Eq. (6) is shown in Eq. (7).

$$\Delta X(t) = X_{rabbit}(t) - X(t) \tag{7}$$

Eqs. (6) and (7) define the soft encircling model during the HHO exploitation phase. If the prey performs a progressive dive, the mathematical expression is shown in Eq. (8).

$$\begin{cases} Y = X_{rabbit}(t) - E \mid JXX_{rabbit}(t) - X(t) \mid \\ Z = Y + S \cdot LF(V) \end{cases} \tag{8}$$

In Eq. (8), S represents a random vector. V is the problem dimension. LF denotes the Lévy flight step size.

3.2. Transportation Route Optimization Model Based on NSGA2-HHO and IPSO-WRF

The core of this study is to solve a multi-objective path optimization problem that balances total logistics cost, product freshness loss, and delivery timeliness. Let x_{ij}^k be a binary variable. If vehicle k travels from node i to node j, it is 1; otherwise, it is 0. The objective function for minimizing total logistics cost is given by Eq. (9).

$$F_1 = \sum_k \sum_i \sum_j (c_{ij}^d + c_{ij}^f)\, x_{ij}^k + \sum_i p_i \cdot max(0, t_i - l_i) \tag{9}$$

In Eq. (9), c_{ij}^d is the driving cost, c_{ij}^f is the fixed vehicle usage cost, p_i is the penalty coefficient for delay at node i, t_i is the time when the vehicle arrives at node i, and l_i is the promised delivery time. The objective function for minimizing freshness loss is shown in Eq. (10).

$$F_2 = \sum_i \sum_k q_i \cdot exp(-\alpha \cdot t_i) \cdot (1 - x_{0i}^k) \tag{10}$$

In Eq. (10), l_i is the initial mass value of the goods at node i, l_i is the decay rate constant, and l_i ensures that the journey from the warehouse is only counted. The objective function of minimizing the total delivery delay is shown in Eq. (11).

$$F_3 = \sum_i max(0, t_i - l_i) \tag{11}$$

The constraints of the model mainly include: each customer point must be accessed and served only once; The total cargo capacity of each delivery vehicle on its driving path shall not exceed its rated capacity limit; The time for the vehicle to arrive at any node must meet the dual constraints of the earliest service time and the latest service time. NSGA2-HHO achieves efficient Pareto front search. However, the dynamic nature of cross-border fresh product transportation requires strong real-time prediction ability for route decision-making. Weighted Random Forest (WRF) captures complex interactions between factors in the transportation route by constructing multiple decision trees. It also improves prediction accuracy through a feature-importance-weighting mechanism that identifies and strengthens the influence of key factors (Rhodes et al., 2023). The WRF flowchart is shown in Fig. 4.

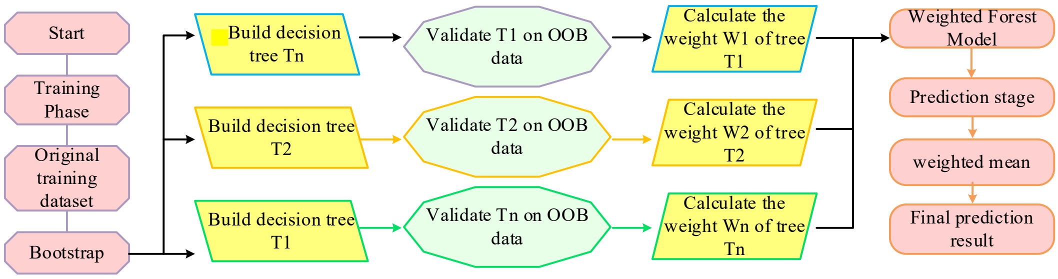

Fig. 4. WRF flowchart (source: author self-drawn)

In Fig. 4, during training, WRF first performs Bootstrap sampling on the original dataset to generate multiple subsets. Then, it builds decision trees based on these subsets. After evaluating each tree with out-of-bag data, the algorithm calculates the corresponding weight for each tree. All decision trees and their weights are integrated into a weighted forest model. In the prediction phase, WRF inputs a new sample, generates prediction results from each decision tree, and aggregates the results through weighted voting or weighted averaging. The equation for calculating weights in a regression task is shown in Eq. (12).

$$W_a = \frac{1}{MSE(T_a)+\varepsilon} \tag{12}$$

In Eq. (12), $MSE(T_a)$ represents the mean squared error of tree T_a on the out-of-bag data. ε is an exceedingly small normal number set to prevent zero division, usually set to 1e-6. It can effectively prevent numerical overflow in weight calculation when $MSE(T_a)$ approaches zero, and will not cause significant bias in weight allocation. The equation for calculating the weighted score of class b during the prediction phase is shown in Eq. (13).

$$Score(b) = \sum_{a=1}^{n} W_a \cdot \prod(T_a(C) = b) \tag{13}$$

In Eq. (13), $\prod$ is an indicator function. The final predicted class in WRF is shown in Eq. (14).

$$A = \arg\max_{b} Score(b) \tag{14}$$

In Eq. (14), A represents the class with the highest score. WRF has limitations in precisely optimizing parameters and tends to lose balance in weight distribution when overseeing complex data. The Improved Particle Swarm Optimization (IPSO) improves WRF by adjusting weights and selecting features using swarm intelligence. It also accelerates training with parallel computation, enhancing WRF performance in complex tasks (Yang et al., 2022). IPSO optimizes WRF to form the hybrid algorithm IPSO-WRF. The IPSO-WRF flowchart is shown in Fig. 5.

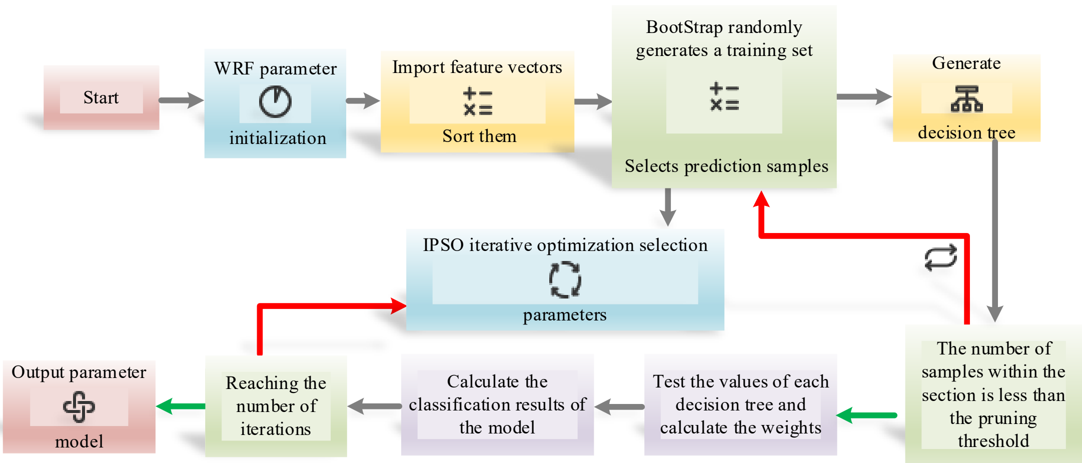

Fig. 5. IPSO-WRF hybrid algorithm flowchart (source: author self-drawn)

As shown in Fig. 5, the process begins with initializing WRF parameters. Then, the algorithm imports and ranks feature vectors. Using the Bootstrap method, it samples data, generates training sets, and selects prediction samples. If the number of samples in a node is smaller than the pruning threshold, it evaluates the decision trees and calculates their weights. If the sample size is not below the threshold, the algorithm returns to the sampling step to ensure proper tree construction. If the result reaches the preset number of iterations, the model parameters are output. The mathematical equation for IPSO is given by Eq. (15).

$$\begin{cases} v_{jg}^{k+1} = wv_{jg}^{k} + s_1 u_1 (P_{jg}^{k} - X_{jg}^{k}) + s_2 u_2 (P_{hg}^{k} - X_{jg}^{k}) \\ X_{jg}^{k+1} = X_{jg}^{k} + v_{jg}^{k+1} \end{cases} \tag{15}$$

In Eq. (15), v_{jg}^{k+1} represents the velocity of a particle j in the g -th dimension after the j -th iteration. w is the inertia weight. s is a non-negative acceleration coefficient. r is a random number between 0 and 1. P_{jg}^{k} and X_{jg}^{k} are the individual best position and current position of particle j in the g -th dimension after the k -th iteration. P_{hg}^{k} is the global best position of the swarm in the g -th dimension after the k -th iteration. NSGA2-HHO combines multi-objective optimization with efficient global search to generate diverse, high-quality solutions. IPSO improves WRF by enhancing its feature handling and prediction capabilities. The integration of these two algorithms results in a transportation route optimization model based on NSGA2-HHO and IPSO-WRF. The flowchart of the combined optimization model is shown in Fig. 6.

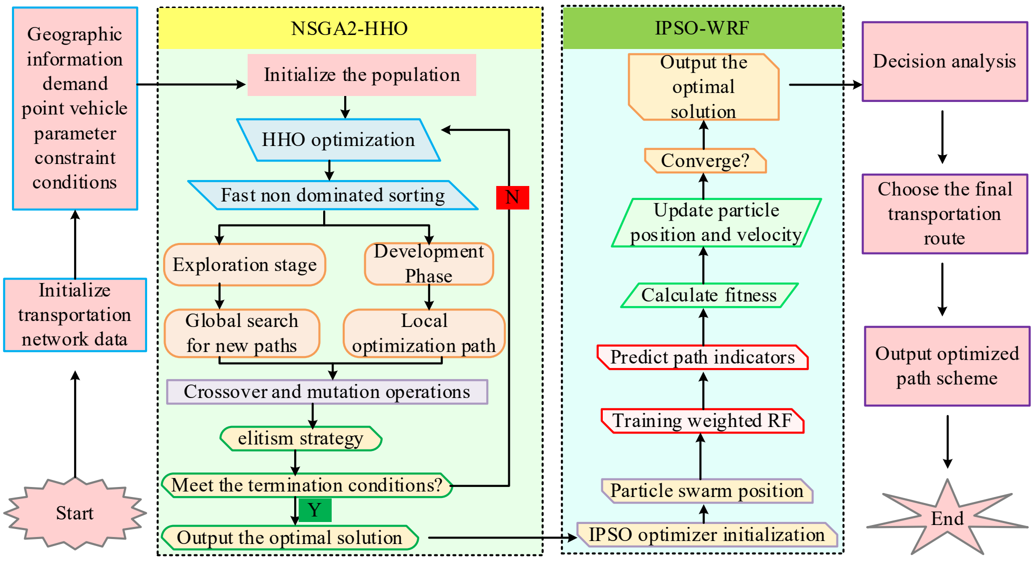

Fig. 6. Combined optimization model of NSGA2-HHO and IPSO-WRF (source: author self-drawn)

As shown in Fig. 6, the model first initializes transportation network data. After entering the parameters and constraints, it proceeds to the NSGA2-HHO optimization module. To achieve the dual objectives of "global optimization+dynamic response," NSGA2-HHO searches for a set of multi-objective optimal paths on a global scale to form the initial Pareto front. IPSO-WRF conducts real-time evaluation and fine-tuning of each path based on this, predicts its performance in the current environment through WRF, and provides feedback on adjustment suggestions. If the external environment changes, IPSO-WRF triggers a reassessment and feeds back the updated path score to NSGA2-HHO, guiding it to prioritize the path with stronger adaptability in the next iteration. In terms of interface design, the Pareto optimal solution set output by the NSGA2-HHO module is used as input to the IPSO-WRF module. The IPSO-WRF module receives these solutions and predicts the transportation time and quality loss of each path based on dynamic factors such as real-time traffic data and weather conditions. In terms of data stream transmission, the two modules interact with each other through structured data tables, and the data transmission adopts memory sharing to ensure efficient interaction. In addition to overcoming the limitations of insufficient consideration of randomness in existing research, this study introduces a probability distribution model to model the customs clearance process explicitly. The customs clearance time is modeled as a log-normal distribution based on historical data, and its probability density function is shown in Eq. (16).

$$f(t) = \frac{1}{t\sigma\sqrt{2\pi}} \times exp[-\frac{(ln(t)-\mu)^2}{2\sigma^2}] \tag{16}$$

In Eq. (16), μ and σ are parameters fitted based on different ports, types of goods, and historical customs clearance records. The customs clearance results are modeled using a polynomial distribution, and their probabilities are dynamically updated through machine learning methods. During path optimization, the IPSO-WRF module uses the customs clearance status as a key dynamic feature. In each decision-making cycle, the system generates multiple random scenarios based on the probability distribution of the current customs clearance status, evaluates the performance of each path scheme across these scenarios, and generates robust path decisions.

4. Performance Analysis of Transportation Route Optimization Model Based on NSGA2-HHO and IPSO-WRF

4.1. Validation of NSGA2-HHO Multi-Objective Algorithm

To evaluate the effectiveness of the NSGA2-HHO multi-objective algorithm, the study compared it with Multi-Objective

Particle Swarm Optimization (MOPSO), NSGA2, and Improved Harris Hawks Optimization (IHHO). The experimental system ran Windows 10 with Linux 5.15.133. The programming language was C++, and the development environment was Vivado 2012.2. The simulation used an NVIDIA A100 CPU with 16GB of memory. To ensure the reliability of the experimental results, the Fashion-MNIST dataset was selected. The Fashion MNIST dataset is a publicly available benchmark for image classification, consisting of 60,000 grayscale images with high-dimensional features and complex patterns. It can effectively assess the generalization search and convergence stability of the NSGA2-HHO algorithm in unstructured data spaces. To verify the effectiveness of NSGA2-HHO, the study compared its recall rate against confidence levels with those of MOPSO, NSGA2, and IHHO. Set the population size to 100, the maximum number of iterations to 200, the crossover probability to 0.9, and the mutation probability to 0.1. In the HHO section, the initial energy is randomly generated within [-1,1], and the energy decay coefficient during iteration is 2. All algorithms use the same termination conditions to ensure fair comparison. The results appeared in Fig. 7.

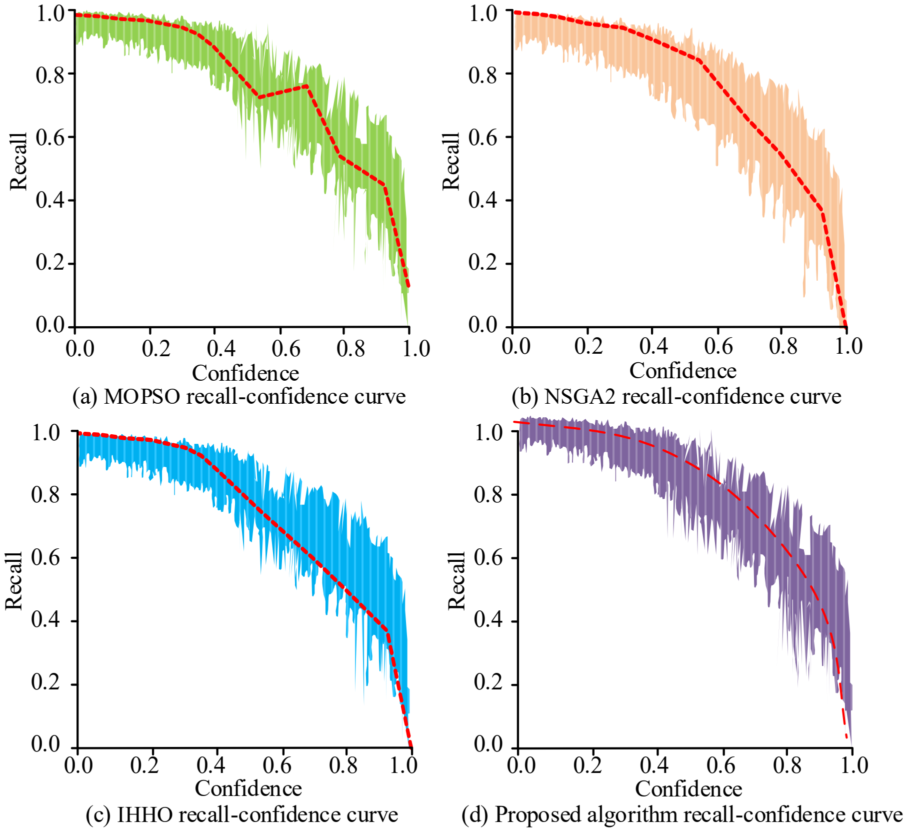

Fig. 7. Recall rate comparison of four algorithms (source: author self-drawn)

In Fig. 7(a), as the confidence level increases, the recall rate of MOPSO decreases sharply. Fig. 7(b) showed NSGA2 with a recall rate of around 0.8 at a confidence of 0.3, which dropped to about 0.5 when the confidence reached 0.7. In Fig. 7(c), IHHO demonstrated a recall rate of around 0.8 at a confidence of 0.4, which fell to around 0.3 when the confidence rate was 0.8. Fig. 7(d) displayed the proposed algorithm with a recall rate of approximately 0.7 at a confidence of 0.6, outperforming the other models at the same confidence level. In summary, the proposed algorithm maintained a relatively high recall rate even at higher confidence levels. To further validate the effectiveness of NSGA2-HHO, the study compared the accuracy and loss rates, as shown in Fig. 8

In Fig. 8(a), the proposed algorithm's accuracy rapidly increased to 88.9% before 120 iterations, then grew steadily. At 150 iterations, accuracy reached 90.0% and continued to rise slowly, with an average accuracy of 94.8%. NSGA2 showed rapid early growth, with a stable accuracy of 88.5%. Fig. 8(b) shows that the loss sharply decreased to 0.54% within the first 50 iterations, then steadily converged at about 0.08 per 50 iterations, ending with a final loss of 0.018% and an average loss rate of 0.023%, better than the other algorithms. Overall, the proposed algorithm showed significant advantages in both accuracy and loss control.

4.2. Validation of IPSO-WRF Hybrid Algorithm

After confirming NSGA2-HHO's effectiveness, the study further validated the accuracy of the IPSO-WRF hybrid algorithm. The experimental environment remained consistent: Windows 10, Linux 5.15.133, C++, Vivado 2012.2, NVIDIA A100 CPU, and 16GB memory. Determine parameter settings through grid search and pre-experiments, set the particle swarm size to 50, the maximum iteration number to 100, the cognitive factor c1 and social factor c2 to 1.5, and use a linear decreasing strategy to reduce inertia weight from 0.9 to 0.4. The number of decision trees in WRF is set to 100, the maximum depth is 15, and the weighted threshold for feature importance is set to 0.01. To prevent overfitting, 10-fold cross-validation is used for early stopping. The study compared the recognition precision-recall curves of NSGA2-HHO, MOPSO, IPSO, and WRF algorithms across four datasets. The results are shown in Fig. 9.

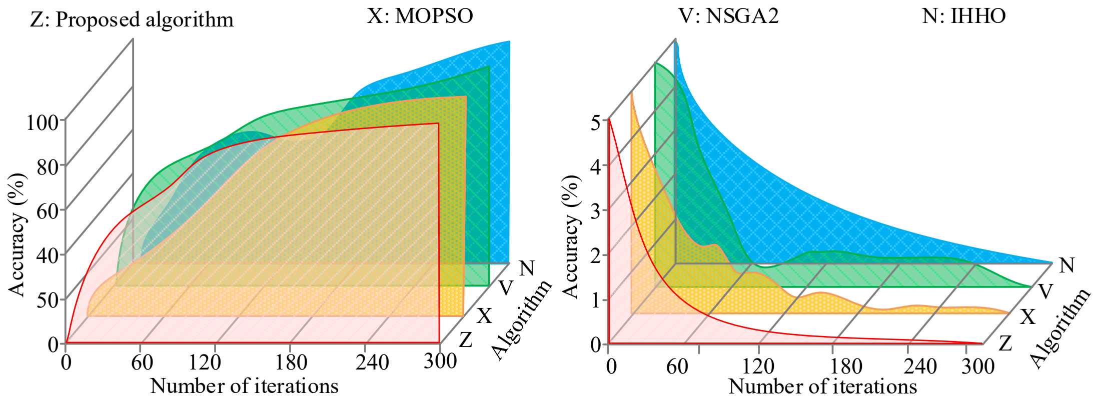

(a) Comparison chart of accuracy curves
(b) Comparison chart of loss curves

Fig. 8. Accuracy and loss comparison of four algorithms (source: author self-drawn)

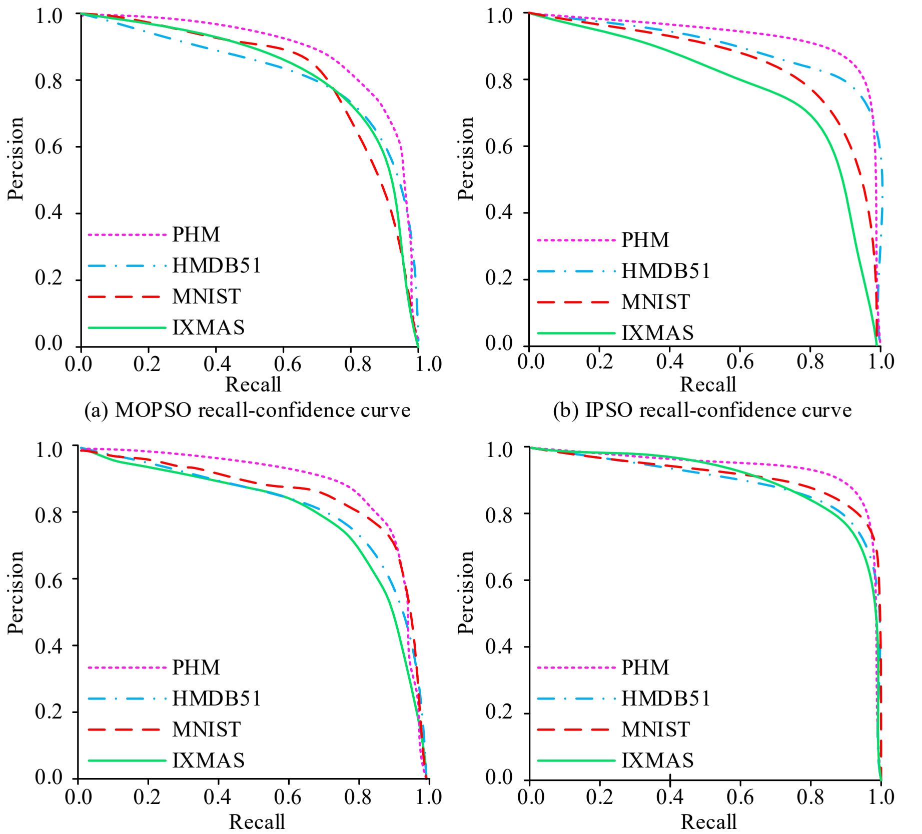

(a) MOPSO recall-confidence curve
(b) IPSO recall-confidence curve
(c) WRF recall-confidence curve
(d) Proposed algorithm recall-confidence curve

Fig. 9. Recognition precision-recall curves of four algorithms (source: author self-drawn)

In Fig. 9(a), when recall was 0.81, the accuracy of MOPSO only reached 0.42. Fig. 9(b) indicates that IPSO achieved a precision of 0.55 at a recall of 0.8 on the MNIST dataset but performed worse on IXMAS. Fig. 9(c) revealed WRF's precision at a recall of 0.8 on HMDB51 and MNIST datasets was 0.68 and 0.65, respectively. Fig. 9(d) demonstrated that the proposed algorithm had the best overall performance, achieving a precision of 0.85 at a recall of 0.8 on PHM and precisions of 0.76 and 0.74 on HMDB51 and MNIST, respectively. To further verify the effectiveness of the IPSO-WRF hybrid algorithm, the study conducted loss convergence tests comparing it with MOPSO, IPSO, and WRF, as shown in Fig. 10.

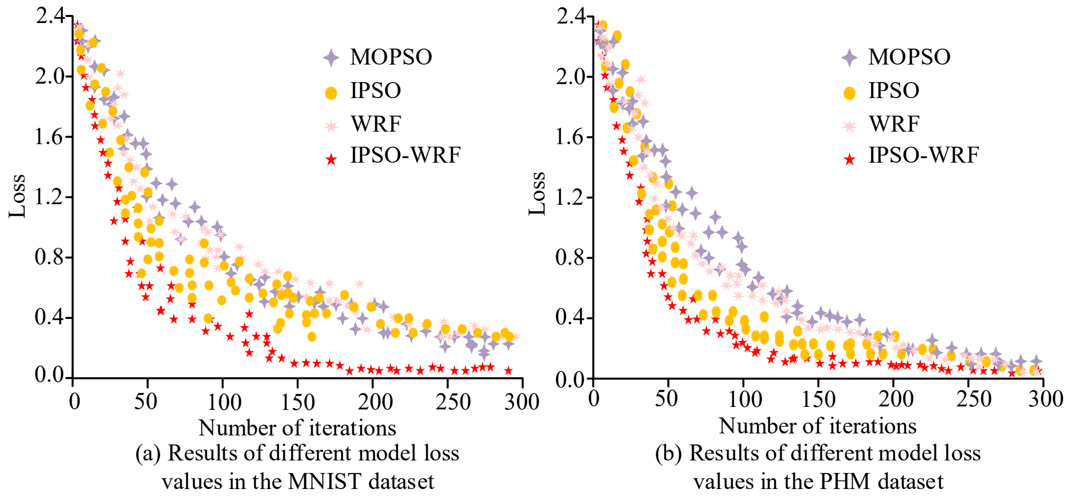

Fig. 10. Loss convergence tests of four algorithms on different datasets (source: author self-drawn)

Fig. 10(a) shows that on the MNIST dataset, the proposed model's loss decreased rapidly as iterations progressed, dropping significantly by 50 iterations and approaching zero after over 200 iterations. Fig. 10(b) shows that, in the PHM dataset, the proposed model converged faster to a lower loss value. After 150 iterations, the loss was nearly 0.2, while other models still maintained higher loss values. Overall, the proposed model showed better convergence across both datasets, leading to greater loss reduction. This indicated a more efficient training process and faster stabilization at a low-loss state, outperforming the other three models.

4.3. Application Evaluation of Proposed Transportation Route Optimization Model

After validating the effectiveness of the NSGA2-HHO multi-objective model and the IPSO-WRF hybrid algorithm, the study further evaluated a transportation path optimization model that combined the two. The study compared this model with IHHO, IPSO, and WRF using the Area Under the ROC Curve (AUC) and the F1 score. The experimental results are shown in Fig. 11.

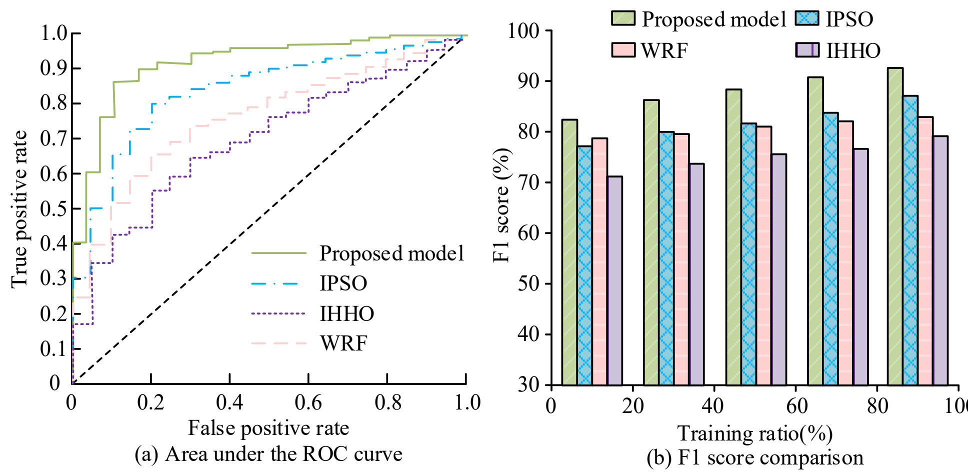

Fig. 11. ROC curves and F1 score comparison (source: author self-drawn)

As shown in Fig. 11(a), the ROC curve of the proposed model was closest to the top-left corner, and its AUC was 0.89, the highest and significantly higher than those of the comparison models (0.85, 0.79, and 0.72). This indicated better classification performance and more reliable prediction results. Fig. 11(b) showed that the F1 scores of the proposed model all exceeded 80%, which was notably higher than those of the other models, further confirming its classification capability. To verify the practical application performance of the proposed model, the study compared the satisfaction of its optimal solutions across different seasons with those of IHHO, IPSO, and WRF. The results are presented in Table 1.

As shown in Table 1, the proposed model demonstrated consistent satisfaction with timeliness throughout the year. In spring, the satisfaction rate reached 92.3%, followed by 95.4% in summer, 91.2% in autumn, and 89.7% in winter. The annual average satisfaction for time was as high as 92.2%. In terms of quality satisfaction, the proposed model achieved more than 93% across all seasons: 93.6% in spring, 95.1% in summer, 93.1% in autumn, and 95.1% in winter. The annual average quality satisfaction reached 94.3%, which was superior to the other models. Overall, the proposed model demonstrated remarkable robustness across seasons. To further validate the model's generalization ability, extension experiments were conducted on the Solomon VRPTW benchmark dataset (C101), and the proposed model was compared with Deep Q-Network (DQN), Graph Neural Network (GNN), Ant Colony Optimization (ACO), and Genetic Algorithm (GA). Using total path length, runtime, and memory consumption as evaluation metrics. The performance comparison results of the five methods are shown in Table 2.

Table 1. Optimal solution satisfaction results (%)

Model	Season	Proposed model	IHHO	IPSO	WRF
Time satisfaction	Spring	92.3	77.5	87.5	81.5
	Summer	95.4	79.4	66.4	72.6
	Autumn	91.2	76.8	52.1	61.7
	Winter	89.7	88.1	83.5	85.8
Annual average satisfaction	/	92.2	80.5	72.4	75.4
Quality satisfaction	Spring	93.6	77.1	61.5	74.9
	Summer	95.1	76.2	79.7	88.7
	Autumn	93.1	84.5	65.6	65.6
	Winter	95.1	78.6	74.6	76.7
Annual average satisfaction	/	94.3	79.1	70.4	76.4

Table 2. Performance comparison results of five methods

Methods	Path length/km	Runtime/s	Memory consumption/MB
DQN	854.4	128.5	892
GNN	836.9	53.0	685
ACO	847.3	89.4	258
GA	858.7	62.3	297
NSGA2-HHO and IPSO-WRF	828..4	46.2	315

As shown in Table 2, the proposed model yielded the shortest path length (828.4 km) and the shortest running time (46.2s). Although the memory consumption is slightly higher than ACO and GA, it is significantly lower than deep learning methods, achieving a better balance between solution quality and computational resource consumption. To verify the performance of the model in sudden abnormal situations, this study injected two customized extreme testing scenarios based on the Solomon R series standard dataset: customs delay (randomly selecting 30% of customer points, extending service time by 100-300% to simulate customs clearance delay) and regional traffic interruption (randomly prohibiting 15% of path node access to simulate road closure). Compare the proposed model with three typical multi-objective algorithms: MOPSO, NSGA3, and Strength Pareto Evolutionary Algorithm 2 (SPEA2). The total path cost increase rate, time window violation rate, and CPU time increase rate were used as evaluation indicators, and the average of 20 independent experiments was taken as the result. The performance comparison results of four algorithms under extreme disturbance scenarios are shown in Table 3.

Table 3. Performance Comparison of Four Algorithms in Extreme Disturbance Scenarios

Extreme scenario	Algorithms	Total path cost increase rate/%	Time window violation rate/%	CPU time increase rate/%
Customs delay	MOPSO	25.4	22.4	28.9
	NSGA3	21.8	18.7	23.7
	SPEA2	23.2	20.5	25.4
	NSGA2-HHO and IPSO-WRF	12.4	8.7	15.3
Traffic interruption	MOPSO	32.7	28.9	35.2
	NSGA3	27.6	23.8	29.9
	SPEA2	29.2	25.5	31.7
	NSGA2-HHO and IPSO-WRF	15.7	12.3	18.8

As shown in Table 3, under two extreme disturbance scenarios, the proposed model has the lowest total path cost increase rate, time window violation rate, and CPU time increase rate, all of which do not exceed 20%, and can quickly generate feasible optimization paths when the environment suddenly changes.

4.4. Examples of Practical Applications and Data Integration

To adapt the model to dynamic environments, it is necessary to integrate real-time data from multiple sources. Traffic congestion data is obtained from map APIs such as Amap and Google Maps to provide real-time travel times for road segments. Weather data is extracted from meteorological service interfaces (such as OpenWeatherMap) and converted into impact coefficients on driving speed and cargo spoilage rate. The customs clearance status is obtained by accessing the port logistics public information platform, obtaining the message status, and using a probability model trained on historical data to predict delays. In practical operation, these real-time data streams are preprocessed into input feature vectors for the IPSO-WRF module. IPSO-WRF immediately predicts the travel time and quality loss of candidate paths at the minute level and feeds the evaluation results back to the NSGA2-HHO module. NSGA2-HHO adjusts individuals fitness in the population based on feedback, thereby generating robust path schemes that are more resistant to real-time disturbances in the next iteration, ultimately achieving a closed-loop decision-making process of "perception prediction optimization".

5. Discussion

To address the complex problem of optimizing transportation paths for fresh products in cross-border e-commerce, this study proposed an optimization model based on a multi-objective framework and a hybrid algorithm. The results showed that the ROC curve of the proposed model was closest to the top-left corner, and its AUC was 0.89, the closest to 1 among all models. In terms of real-world application performance, the model's time satisfaction rate reached 92.3% in spring, 95.4% in summer, 91.2% in autumn, and 89.7% in winter. The annual average time satisfaction reached 92.2%. For quality satisfaction, the model achieved 93.6% in spring, 95.1% in summer, 93.1% in autumn, and 95.1% in winter. The annual average quality satisfaction reached 94.3%, significantly higher than that of the comparison models.

The computational complexity of this model primarily arises from two components: the multi-objective optimization with NSGA2-HHO and the real-time prediction with IPSO-WRF. The complexity of NSGA2-HHO is approximately $O(MN^2)$, where M is the target number (3 in this study), and N is the population size. The introduction of HHO does not change the overall complexity level but increases the computational cost of individual updates per generation. The complexity of the prediction stage of IPSO-WRF depends on the number and depth of decision trees in the random forest, as well as the number of iterations of particle swarm optimization. In the Solomon C101 benchmark test, the model's average runtime was 46.2s, indicating its practical efficiency on medium-sized problems. However, for large-scale logistics networks (with more than 500 nodes), the computational complexity of non-dominated sorting and crowding in NSGA2 will increase significantly as the population and disaggregation sizes grow, posing challenges to the model's scalability. Therefore, scalability can be improved in the future by introducing hierarchical optimization strategies or by adopting distributed computing frameworks such as Spark to parallelize population evaluation. In addition, feature selection and model simplification in IPSO-WRF can be further optimized to balance prediction accuracy and computational time.

6. Conclusion

In summary, the proposed transportation path optimization model, based on a multi-objective framework and a hybrid algorithm, effectively addressed the limitation of traditional genetic algorithms, which can fall into local optima. The core contribution of the proposed model lies in the synergy of multi-objective global optimization and dynamic response mechanism, which provides a new method for solving complex decision-making problems in cross-border fresh food logistics. In normalized logistics planning, it can generate Pareto-optimal path solutions that balance cost, timeliness, and quality using historical data. In a dynamic operating environment, it can perform minute-level re-optimization of transportation routes based on real-time traffic and weather data. However, the model still has limitations when facing sudden changes in border policies or extreme weather conditions. Sudden import restrictions or regional traffic paralysis caused by typhoons may pose a risk of failure for current models trained on historical data. Therefore, future research will focus on integrating real-time policy-warning data and meteorological disaster-warning systems into models, combined with online reinforcement-learning mechanisms, to establish rapid-response strategies for emergency situations.

Author Contributions

Zhe Chen contributed to conceptualization, methodology, software, validation, analysis, investigation, data collection, draft preparation, manuscript editing, visualization, supervision, project administration, and funding acquisition. Guangwen Zhang contributed to conceptualization, methodology, software, validation, analysis, investigation, data collection, draft preparation, manuscript editing, visualization, supervision, and project administration.

Funding

This research received no specific financial support from any funding agency.

Institutional Review Board Statement

Not applicable.

Declaration of Artificial Intelligence (AI) Tools

The authors used ChatGPT solely for language editing and to improve readability. The authors reviewed and verified all content and take full responsibility for the accuracy and integrity of the manuscript

References

Abeer, A. N. M. N., Urban, N. M., Weil, M. R., Alexander, F. J., and Yoon, B. J. (2024). Multi-objective latent space optimization of generative molecular design models. *Patterns,* 5(10), 101042–101055.

Bai, L., Liu, M., and Sun, Y. (2023). Overview of food preservation and traceability technology in the smart cold chain system. *Foods,* 12(15), 2881–2930.

Dong, B., Duan, M., Li, Y., Duan, M., and Li, Y. (2022). Exploration of joint optimization and visualization of inventory transportation in agricultural logistics based on ant colony algorithm. *Computational Intelligence and Neuroscience,* 2022(1), 2041592–2041603.

Fahrni, M. L., Ismail, I. A., Refi, D. M., Almeman, A., Yaakob, N. C., Saman, K. M., Mansor, N. F., Noordin, N., and Babar, Z. U. (2022). Management of COVID-19 vaccines cold chain logistics: a scoping review. *Journal of Pharmaceutical Policy and Practice,* 15(1), 16–29.

Guizzo, G., Califano, F., Sarro, F., Ferrucci, F., and Harman, M. (2023). Inferring test models from user bug reports using multi-objective search. *Empirical Software Engineering,* 28(4), 95–135.

He, X., Huanyu, E., and Ding, G. (2023). Development of a CH_2-dependent analytical method using near-infrared spectroscopy via the integration of two algorithms: non-dominated sorting genetic-II and competitive adaptive reweighted sampling (NSGAII-CARS). *Analytical Methods,* 15(10), 1286–1296.

Hussain, M. M., Azar, A. T., Ahmed, R., Umar Amin, S., Qureshi, B., Dinesh Reddy, V., Alam, I., and Khan, Z. I. (2023). SONG: A multi-objective evolutionary algorithm for delay and energy aware facility location in vehicular fog networks. *Sensors,* 23(2), 667–704.

Li, J., Gurgenci, H., Guan, Z., Wang, J., Chen, J., Wang, C., and Huang, Z. (2025). Multi objective optimization algorithm for hybrid quantum harmonic oscillator and its application in rotor system optimization. *Scientific Reports,* 15(1), 7534-7549.

Liu, Y., Wu, F., Liu, Z., Wang, K., Wang, F., and Qu, X. (2023). Can language models be used for real-world urban-delivery route optimization? *Innovation,* 4(6), 100520-100527.

Plewes, K., Khonputsa, P., Day, N. P. J., Lubell, Y. (2023). Cost, health impacts and cost effectiveness of iceless refrigeration in India's last-mile vaccine cold chain delivery. *Transactions of The Royal Society of Tropical Medicine and Hygiene,* 117(4), 310-312.

Ren, X., Chen, S., and Ren, L. (2023). Optimization of regional emergency supplies distribution vehicle route with dynamic real-time demand. *Mathematical Biosciences and Engineering,* 20(4), 7487–7518.

Rhodes, J. S., Cutler, A., and Moon, K. R. (2023). Geometry-and accuracy-preserving random forest proximities. *IEEE Transactions on Pattern Analysis and Machine Intelligence,* 45(9), 10947–10959.

Ru, S. (2024). Vehicle logistics intermodal route optimization based on Tabu search algorithm. *Scientific Reports,* 14(1), 11859–11871.

Ryalat, M. H., Dorgham, O., Tedmori, S., Al-Rahamneh, Z., Al-Najdawi, N., and Mirjalili, S. (2023). Harris hawks optimization for COVID-19 diagnosis based on multi-threshold image segmentation. *Neural Computing and Applications,* 35(9), 6855–6873.

Safia, N. S. (2023). Prediction of breast cancer through random forest. *Current Medical Imaging,* 19(10), 1144–1155.

Sang, Y., Chen, X., Chen, Q., Tao, J., and Fan, Y. (2023). A route planning for oil sample transportation based on improved A* algorithm. *Scientific Reports,* 13(1), 22041–22056.

Wu, X., Yu, L., and Pehrsson, P. R. (2022). Are processed tomato products as nutritious as fresh tomatoes? Scoping review on the effects of industrial processing on nutrients and bioactive compounds in tomatoes. *Advances in Nutrition,* 13(1), 138–151.

Yang, L., Ding, B., Liao, W., and Li, Y. (2022). Identification of preisach model parameters based on an improved particle swarm optimization method for piezoelectric actuators in micro-manufacturing stages. *Micromachines,* 13(5), 698–708.

Zhang, F., Wen, B., Niu, D., Li, A., and Guo, B. (2024). Optimized Design of Low-Carbon Mix Ratio for Non-Dominated Sorting Genetic Algorithm II Concrete Based on Genetic Algorithm-Improved Back Propagation. *Materials,* 17(16), 4077–4094.

Zhang, Z., Lin, X., and Wu, S. (2023). A hybrid algorithm for clinical decision support in precision medicine based on machine learning. *BMC Bioinformatics,* 24(1), 3–20.

Zhe Chen earned her bachelor’s degree in business administration from Harbin University of Commerce in 2006 and her master’s degree in political economy from Southwest University in 2010. Since 2014, she has been teaching at Heilongjiang Polytechnic, specializing in e-commerce and new media. Her professional experience includes serving as an Administrative Secretary at Sanya University (2010–2013) and as a Deputy Manager of the Planning Department at Tianya Haijiao Tourism Development Co., Ltd. in Sanya (2013–2014). Her research focuses on e-commerce operations and promotion, new media operations, and ice-and-snow talent training. She has authored four academic works and textbooks, led three provincial-level research projects, holds two utility model patents, and has received one academic award.

Guangwen Zhang, female, born in April 1985, Han ethnicity, Harbin, Heilongjiang Province. She graduated from Harbin University of Science and Technology with a Bachelor of Arts degree in Japanese Language in 2008, and obtained a Master of Economics degree from Fuji University in 2013. 2013-2017 Teller Harbin Branch, Harbin Bank Co., Ltd. 2017-Present Heilongjiang Polytechnic, Teacher. She has published 1 academic textbook, 1 provincial-level research project, 2 utility model patents.